

Advances of Diagnostic Imaging Related to Progress in Multidetector-row CT Scanners: Impact on the Evaluation of Vascular Diseases

Hiromitsu Hayashi, Ryo Takagi, Katsuya Takahama, Toshihide Kaizu, Nobuyuki Tateno,
Shigehiko Kuribayashi, Fumitaka Hidaka, Hisashi Yoshihara, Hidetaka Sato, and Tatsuo Kumasaki

Abstract: We investigated patients who underwent CT angiography of major or peripheral vascular diseases multiple times using MDCT scanners with a different number of X-ray detector-rows to evaluate the impact of advances of diagnostic imaging from a clinical perspective.

The image quality of main vascular lesions including thoracic aortic aneurysm, abdominal aortic aneurysm, aortic dissection and peripheral arterial disease, and major branch vessels was assessed by a 5-grade scale for subjective comparison of CT angiographies between 16-channel MDCT and 4-channel or 8-channel MDCT. The mean dose of contrast medium for CT angiography was also compared between 16-channel MDCT and 4-channel or 8-channel MDCT.

In conclusion, this study showed that the MDCT scanner is capable of acquiring volume data sets that provide excellent longitudinal spatial resolution in a shorter scan time due to the increase of X-ray detector-rows. Sixteen-channel MDCT provides clear and artifact-free CT angiography of major aortic lesions as well as peripheral arterial disease. Sixteen-channel MDCT was particularly superior to fewer-channel MDCT in terms of the capability to visualize small arteries. In addition, not only the volume of contrast medium but also calculated CT radiation dose of the same examination distance tended to decrease as scanning time shortened, suggesting that an advanced MDCT scanner could promote further reduction in invasiveness of CT examination. (J Jpn Coll Angiol, 2005, 45: 597–606)

Key words: multidetector-row CT, multislice CT, CT angiography, vascular disease

Introduction

A multidetector-row CT (MDCT) scanner is a CT apparatus with multiple X-ray detector-rows mounted in the longitudinal direction in the gantry of a CT scanner. MDCT scanners are capable of acquiring imaging data of multiple slices simultaneously during one rotation of the X-ray tube.^{1,2} With the MDCT scanner, it is possible to obtain greater volume coverage with higher spatial and temporal resolution during a shorter scan time, compared with a helical CT scanner with a single X-ray detector-row.³⁻⁵ After the introduction of a

4-channel (4-ch) MDCT scanner in 1998, 8-channel and then 16-channel MDCT scanners (8- and 16-ch MDCT, respectively) were developed over about 5 years. With the 16-ch MDCT scanner, the width of each X-ray detector has been changed to the submillimeter level and it is also possible to use a wider X-ray beam. These features allow 16-ch MDCT to acquire volume data and to achieve very high spatial resolution imaging in a shorter examination time. However, the advances in diagnostic imaging related to such progress of MDCT scanners have not been well evaluated.

We conducted a study to assess the impact of the increase in the number of X-ray channels of a MDCT scanner on

Department of Radiology and Center for Advanced Medical Technology, Nippon Medical School, Tokyo, Japan

Received April 12, 2005 Accepted June 28, 2005

vascular imaging from a clinical perspective. The study involved patients with diverse vascular lesions including aortic and peripheral arterial disease (PAD) who underwent CT angiographies (CTAs) several times using MDCT scanners with a different number of X-ray detector-rows.

Patients and Methods

We used LightSpeed QX/i (GE), a 4-ch MDCT scanner from November 1999 to March 2002; LightSpeed Ultra (GE), an 8-ch MDCT scanner from April 2002 to December 2002; and LightSpeed Ultra 16 (GE), a 16-ch MDCT scanner from January 2003 to date.

The following acquisition parameters were used for the QX/i: a detector configuration of 2.5 mm × 4, helical pitch of 1.5, and table speed of 18.75 mm/s. For the Ultra, a detector configuration of 2.5 mm × 8, helical pitch of 1.35, and table speed of 54 mm/s. For the Ultra 16, a detector configuration of 1.25 mm × 16, helical pitch of 1.375, and table speed of 55 mm/s. Under these acquisition parameters, the examination time for scanning a distance of 30 cm was 16, 5.5, and 5.5 seconds, respectively. Calculated CT dose index (CTDI_{vol}) with previously mentioned acquisition parameters with X-ray tube current of 350 mA was 27.9, 14.9, and 8.9 mGy, respectively. A nonionic iodine contrast medium (Omnipaque 350; Daiichi Pharmaceutical Co., Ltd.) was employed for contrast enhancement. An automated injector was used to administer 100 mL of contrast medium at a rate of 3 mL/second. Scanning was initiated after automatic detection of contrast agent bolus in the region of interest (ROI). For CTA of the thoracic aorta and the entire aorta, the ROI was set to the midportion of the descending thoracic aorta. For CTA of the abdominal aorta and the peripheral arteries from the pelvis to the lower extremities, the ROI was set at the most cranial portion of the abdominal aorta.

Volume data sets acquired with the QX/i or Ultra were reconstructed with a 2.5-mm slice thickness and 1.25-mm slice interval, while Ultra 16 data were reconstructed with a 1.25-mm slice thickness and 1.25-mm slice interval. The reconstructed images were used as source images to reformat three-dimensional CTA.

There were 32,337 patients who underwent CT scanning during the 5-year study between November 1999 and No-

vember 2004, including 1,130 patients who underwent CTA of the aorta or pelvic and lower extremity arteries. Patients who underwent CTA multiple times with different MDCT scanners were excluded from the study if the acquisition parameters or mode of reconstruction differed from those mentioned above or if a dose of contrast medium varied between MDCT examinations. Finally 35 patients who underwent CTA multiple times using a MDCT scanner with a different number of X-ray detector-rows were enrolled in this study. The interval between CTAs ranged from 1 month to 3.5 years (median: 1 year and 7 months). Evaluation for aortic diseases was done in 20 of the 35 patients and for pelvic/lower extremity lesions in remaining 15. Among the 20 patients underwent CTA of the aorta, thoracic aortic aneurysm (TAA) was found in 6 patients, abdominal aortic aneurysm (AAA) in 7, and aortic dissection (AD) in 7. Among the 6 patients with TAA, 16-ch MDCT was compared with 4-ch MDCT in 4 patients and with 8-ch MDCT in 2. Among the 7 patients with AAA, 16-ch MDCT was compared with 4-ch MDCT in 5 and with 8-ch MDCT in 2. Among the other 7 patients with AD, 16-ch MDCT was compared with 4-ch MDCT in 6 and with 8-ch MDCT in one. CTA of the pelvic/lower extremity arteries was performed for PAD in all 15 patients, and 16-ch MDCT was compared with 4-ch MDCT in 11 of them and with 8-ch MDCT in 4.

The thin section two-dimensional CT images were transferred to an image analysis workstation (Advantage Windows Ver.4.0: GE), where

(1) CTA was reconstructed by both the volume rendering (VR) method and the maximum intensity projection (MIP) method, using a constant level of image reconstruction and display conditions. The obtained CTA images were qualitatively evaluated with respect to visualization of the main vascular lesions and major branches. Visualization of main vascular lesions and major branches were assessed on a 5-grade scale (2, 1, 0, -1, or -2). The criteria for assessment of visualization of main vascular lesions and major branches were defined as follows: "2" meant CTA reconstructed from volume data obtained with 16-ch MDCT scanner was clearly superior to CTA obtained with MDCT scanners with fewer channels (4- or 8-ch) regarding image quality or the

capability to provide diagnostic information, “1” meant CTA with 16-ch MDCT scanner was superior to CTA obtained with MDCT scanners with fewer channels, “0” meant CTA with 16-ch MDCT scanner was equivalent to CTA obtained with MDCT scanners with fewer channels, “-1” meant CTA with 16-ch MDCT scanner was inferior to CTA obtained with MDCT scanners with fewer channels, and “-2” meant CTA with 16-ch MDCT scanner was apparently inferior to CTA obtained with MDCT scanners with fewer channels. The grading was determined by consensus between two radiologists who evaluated the CTA images.

(2) Coronal multiplanar reconstruction (MPR) images were created and evaluated qualitatively with respect to clear delineation of main vascular lesions and major branches. Delineation of main vascular lesions and major branches were assessed on a 5-grade scale (2, 1, 0, -1, or -2).

The criteria for assessing delineation of main vascular lesions and major branches were defined as follows: “2” meant delineation of the vascular lesions on coronal MPR image reconstructed from volume data obtained with 16-ch MDCT scanner was clearly superior to MPR image obtained with MDCT scanners with fewer channels (4- or 8-ch), “1” meant CTA with 16-ch MDCT scanner was superior to MPR image obtained with MDCT scanners with fewer channels, “0” meant CTA with 16-ch MDCT scanner was equivalent to MPR image obtained with MDCT scanners with fewer channels, “-1” meant CTA with 16-ch MDCT scanner was inferior to MPR image obtained with MDCT scanners with fewer channels, and “-2” meant CTA with 16-ch MDCT scanner was apparently inferior to MPR image obtained with MDCT scanners with fewer channels. The grading was determined by consensus between two radiologists who evaluated the CTA images.

(3) CTA images reconstructed by the MIP method with the same window level and window width were evaluated qualitatively with respect to periodic artifacts presenting at muscles and soft tissues. Periodic artifacts presenting at muscles and soft tissues were assessed on a 5-grade scale (2, 1, 0, -1, or -2). “2” meant periodic artifacts with 16-ch MDCT scanner were obviously fewer compared with MDCT scanners with fewer channels (4- or 8-ch), “1” meant periodic artifacts with 16-ch MDCT scanner were fewer com-

pared with MDCT scanners with fewer channels, “0” meant periodic artifacts with 16-ch MDCT scanner were similar compared with MDCT scanners with fewer channels, “-1” meant periodic artifacts with 16-ch MDCT scanner were stronger compared with MDCT scanners with fewer channels, and “-2” meant periodic artifacts with 16-ch MDCT scanner were obviously stronger compared with MDCT scanners with fewer channels. The grading was determined by consensus between two radiologists who evaluated the CTA images.

(4) The dose of contrast medium required to visualize the same volume coverage was compared between 4-, 8-, and 16-ch MDCT scanners.

Statistical analysis was performed with commercially available software (SAS Institute, Cary, NC). Scores were expressed as the mean \pm standard deviation. Visualization scores of main vascular lesions and those of major branches were compared by using the χ^2 exact test. Comparison between the CTAs reconstructed by VR and MIP methods and those with coronal MPR images was performed by using the χ^2 exact test. The results of scores of periodic artifacts between 4- vs 16-ch MDCT scanner and those with 8- vs 16-ch MDCT scanner were also compared by using the χ^2 exact test. $P < 0.05$ was considered to indicate a statistically significant difference.

Results

(1) Detection of main vascular lesions and major branches on CTA images reconstructed by the VR and MIP methods (**Fig. 1**)

Six patients with TAA scored were 0.34 ± 0.47 (mean \pm SD) and 1.34 ± 0.47 for visualization of main vascular lesions and three major branch vessels arising from the aortic arch respectively. There were no significant differences ($p = 0.23$). Seven patients with AAA scored 0.43 ± 0.49 and 1.43 ± 0.49 for detection of main vascular lesions and major branches of the abdominal aorta including celiac axis, splenic artery, common hepatic artery ~ left/right hepatic artery, superior mesenteric artery ~ jejunal artery, and bilateral renal arteries respectively (**Fig. 2**). There were no significant differences ($p = 0.17$). Seven patients with AD scored 0.43 ± 0.49 and 1.29 ± 0.45 for main lesions and major branches including

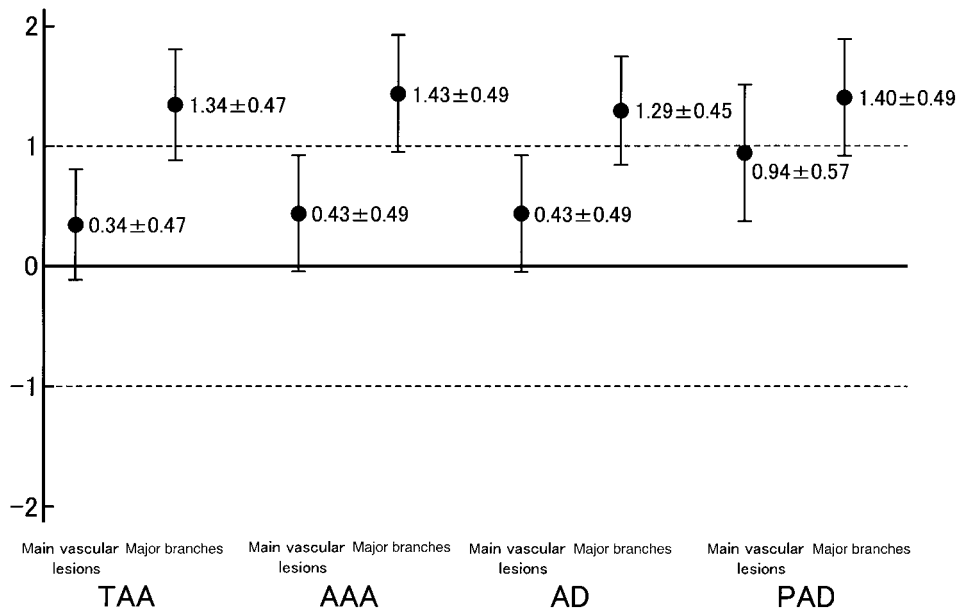


Figure 1 Visual scores of main vascular lesions and major branches on CTA images reconstructed by the VR and MIP methods.

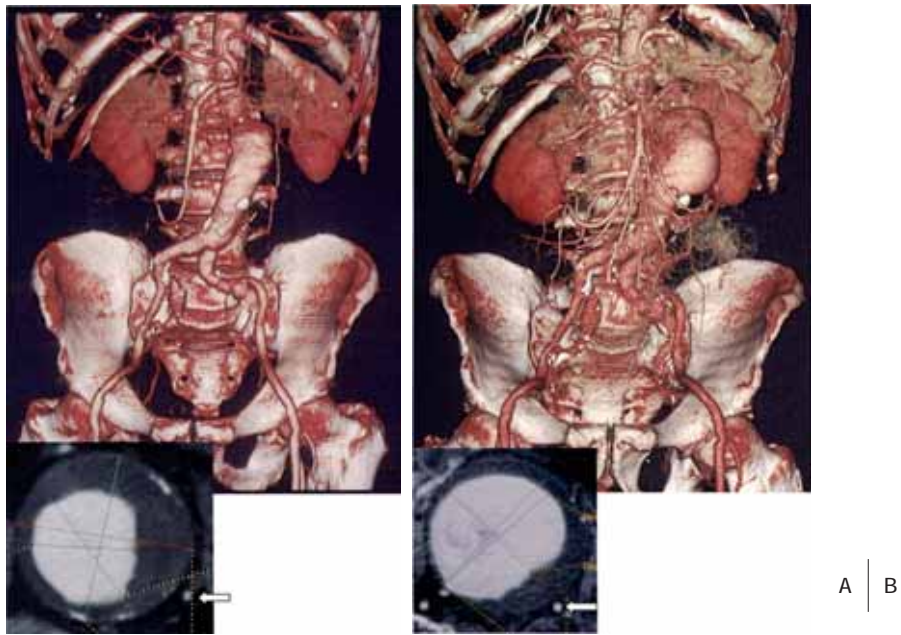


Figure 2 CTA of abdominal aortic aneurysm reconstructed with the VR method (A) and axial CT image (B). A: 4-ch MDCT (Apr 19, 2000).

The CTA image shows a fusiform aneurysm of the abdominal aorta below the origin of the renal arteries. Only the trunks of the main aortic branches are seen. The axial CT image shows blurring of the distal portion of the superior mesenteric artery due to the partial volume effect (arrow).

B: 16-ch MDCT (Jan 31, 2003).

The CTA image shows an enlarged abdominal aortic aneurysm. Not only the main trunks but also the peripheral regions of the main abdominal aortic branches are clearly seen. The axial CT image also nicely shows the distal portion of the superior mesenteric artery (arrow).

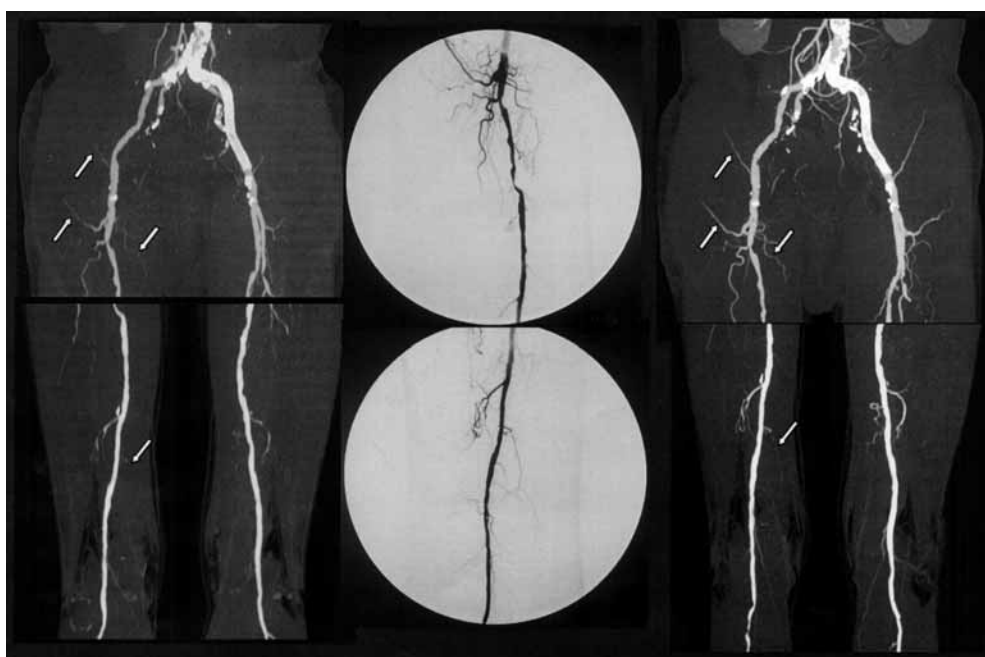


Figure 3 CTA image reconstructed with the MIP method and intraarterial DSA image of peripheral arterial disease.
 A: 8-ch MDCT (Jan 16, 2003).
 The main artery is well visualized, but the branches are not clearly demonstrated (arrows).
 B: Intraarterial DSA image.
 C: 16-ch MDCT (Aug 8, 2003).
 Not only the main artery but also the small branches are very clearly visualized (arrows).
 DSA: digital subtraction angiography

A | B | C

brachiocephalic artery, left common carotid artery, left subclavian artery, celiac axis, superior mesenteric artery, bilateral renal arteries, and common iliac artery respectively. No significant differences were observed ($p = 0.24$). Among the 15 patients undergoing CTA of pelvic/lower extremity arteries for PAD, scores were 0.94 ± 0.57 and 1.40 ± 0.49 with respect to the visualization of arterial stenosis or occlusion and visualization of its major vascular branches including deep circumflex artery, lateral and medial circumflex arteries, deep femoral artery, muscular branches, descending genicular artery, and sural artery, and collateral vessels respectively (**Fig. 3**). There were no significant differences ($p = 0.29$).

(2) Delineation of main vascular lesions and major branches on coronal MPR images (**Fig. 4**)

Six patients with TAA scored 1.17 ± 0.37 (mean \pm SD) and 1.50 ± 0.50 for delineation of the main vascular lesions and three major branch vessels arising from the aortic arch

respectively. No significant differences were observed ($p = 0.83$). Seven patients with AAA scored 1.00 ± 0.53 and 1.43 ± 0.49 for delineation of main vascular lesions and major branches of the abdominal aorta including celiac axis, splenic artery, common hepatic artery ~ left/right hepatic artery, superior mesenteric artery ~ jejunal artery, and bilateral renal arteries respectively. There were no significant differences ($p = 0.63$). Seven patients with AD scored 1.00 ± 0.53 and 1.43 ± 0.49 for main vascular lesions and major branches including brachiocephalic artery, left common carotid artery, left subclavian artery, celiac axis, superior mesenteric artery, bilateral renal arteries, and common iliac artery respectively (**Fig. 5**). No significant differences were observed ($p = 0.88$). In the 15 patients who underwent CTA of the pelvic/lower extremity arteries for PAD, scores were 1.27 ± 0.57 and 1.40 ± 0.49 with respect to the delineation of main vascular lesions and visualization of major vascular branches including deep circumflex artery, lateral and

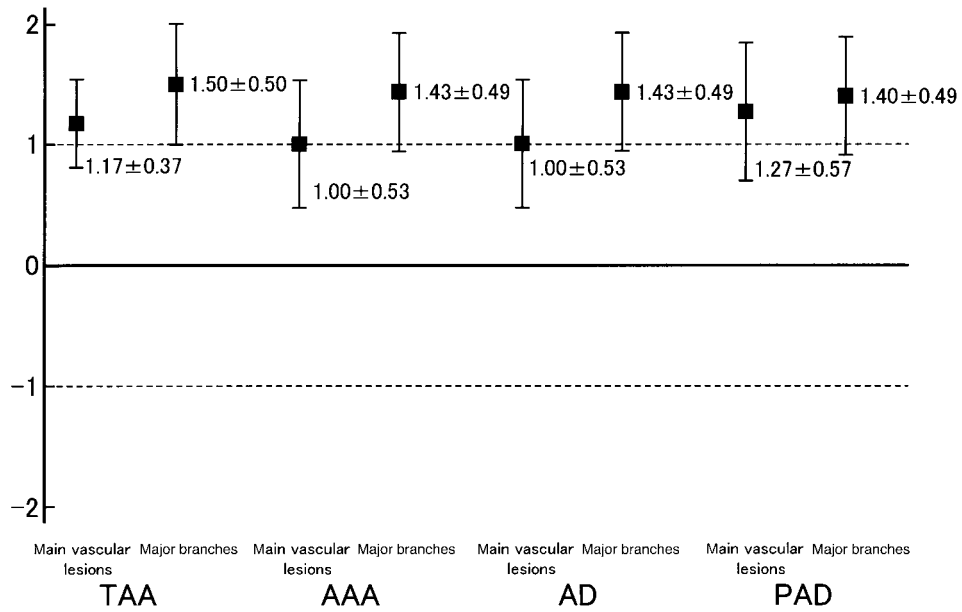


Figure 4 Visual scores of delineation of main vascular lesion and major branches on coronal MPR images.

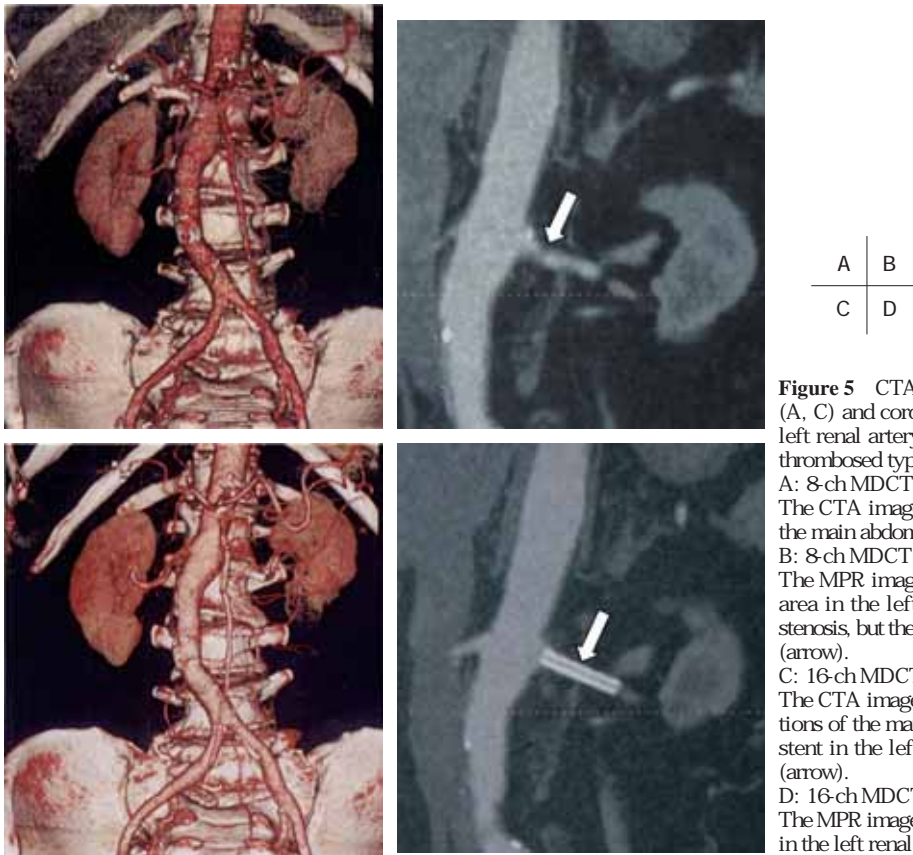


Figure 5 CTA reconstructed with the VR (A, C) and coronal MPR image (B, D) of left renal artery stenosis associated with thrombosed type aortic dissection. A: 8-ch MDCT (VR: Nov 20, 2002). The CTA image only shows the trunks of the main abdominal branches. B: 8-ch MDCT (MPR: Nov 20, 2002). The MPR image shows a low attenuation area in the left renal artery, suggesting stenosis, but the grade of stenosis is unclear (arrow). C: 16-ch MDCT (VR: Jan 16, 2003). The CTA image also shows the distal portions of the main abdominal branches. A stent in the left renal artery can be seen (arrow). D: 16-ch MDCT (MPR: Jan 16, 2003). The MPR image shows patency of the stent in the left renal artery (arrow).

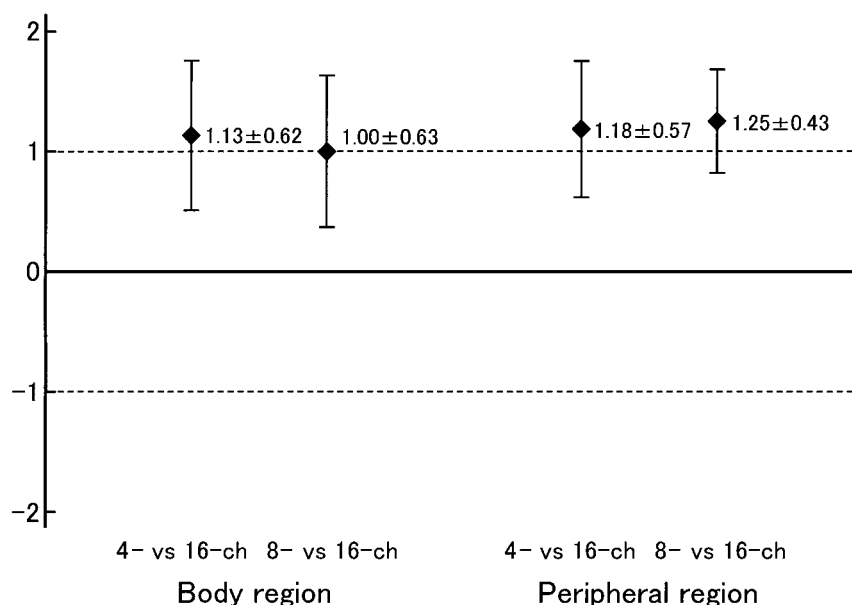


Figure 6 Visual scores of periodic artifacts at muscles and soft tissues on CTA images reconstructed by the MIP method.

medial circumflex arteries, deep femoral artery, muscular branches, descending genicular artery, and sural artery, and collateral vessels respectively. There were no significant differences ($p = 0.97$).

(3) Periodic artifacts at muscles and soft tissues on CTA images reconstructed by the MIP method (Fig. 6)

In terms of the degree of periodic artifacts on CTA images of the aorta (body region), 16-ch MDCT scored 1.13 ± 0.62 points compared with 4-ch MDCT ($n = 15$) and 1.00 ± 0.63 points compared with 8-ch MDCT ($n = 5$) respectively (Fig. 7). There were no significant differences ($p = 0.86$). In terms of periodic artifacts on CTA images of the pelvis/lower extremity arteries (peripheral region), 16-ch MDCT scored 1.18 ± 0.57 points compared with 4-ch MDCT ($n = 11$) and 1.25 ± 0.43 points compared with 8-ch MDCT ($n = 4$) respectively. No significant differences were observed ($p = 0.76$).

(4) Dose of contrast medium for CTA of the same volume coverage

For CTA of the aorta, the mean dose of contrast medium required was 96 mL (92–99 mL) for 4-ch MDCT, 85 mL

(80–90 mL) for 8-ch MDCT, and 82 mL (70–86 mL) for 16-ch MDCT, respectively. For CTA of the pelvic/lower extremity arteries, the mean dose of contrast medium required was 96 mL (90–100 mL) for 4-ch MDCT, 88 mL (92–100 mL) for 8-ch MDCT, and 84 mL (70–88 mL) for 16-ch MDCT, respectively.

Discussion

Since the development of the CT scanner in 1972, exciting advances have been made in association with improvements of computer technology. In this process, the development of helical CT was revolutionary.^{6,7} Breaking away from the previous principles of CT scanning, the helical CT scanner made it possible to collect volumetric data and the capability of continuous X-ray tube rotation with continuous table transport. As a result, volumetric data sets can be obtained with excellent continuity along the Z-axis within a short scanning time, and this novel technology provided in new applications of CT scanning such as CTA.^{8,9} Following the development of the helical CT scanner, the MDCT scanner was developed in 1998. MDCT scanners have multiple X-ray detector-rows mounted in the Z-direction, which enables

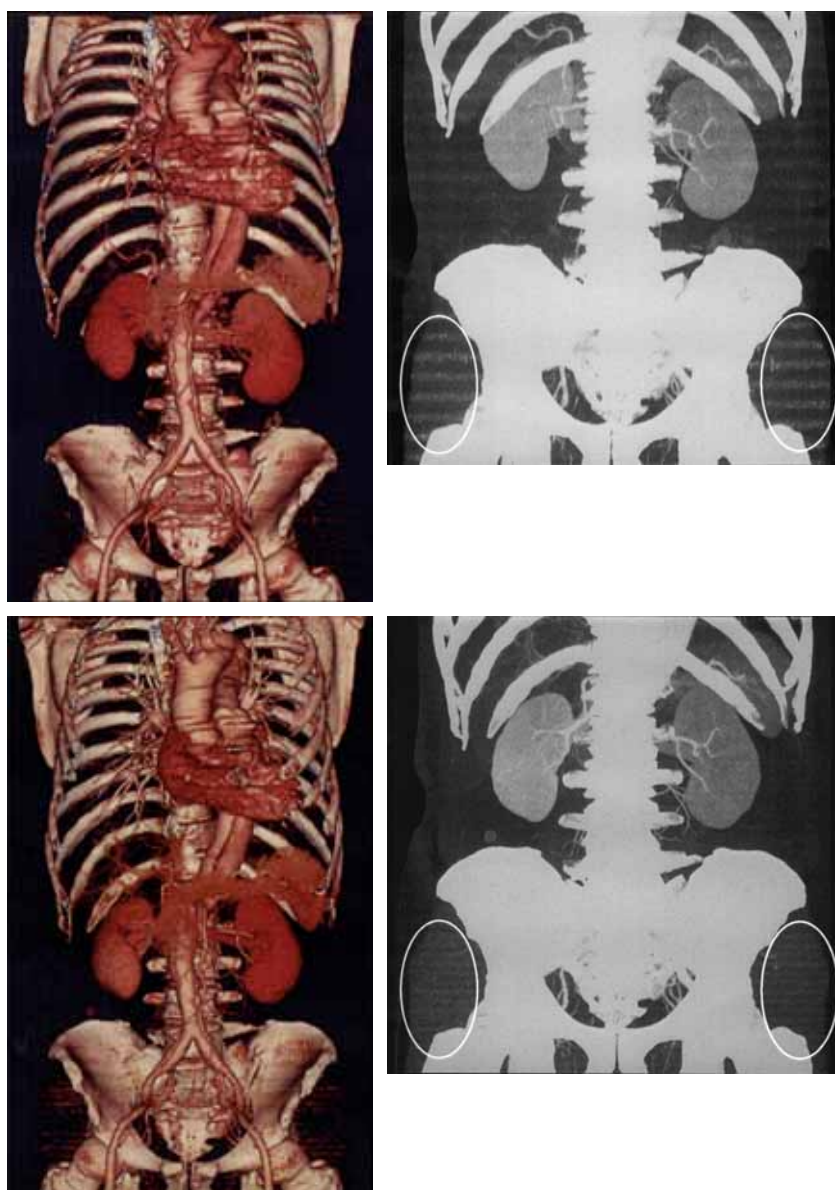


Figure 7 CTA images of patent aortic dissection reconstructed with the VR and MIP methods.
A: 4-ch MDCT (Oct 17, 2001).
The VR image on the left shows a patent aortic dissection from the origin of the left subclavian artery to the bilateral internal iliac arteries. Periodic artifacts at muscles and soft tissues are obvious on the MIP image (ovals).
B: 16-ch MDCT (Feb 6, 2003).
The MIP image on the right shows slight artifacts at muscles and soft tissues (ovals).

simultaneous acquisition of imaging data from multiple slices during one rotation of the X-ray tube.^{1,2} Compared with helical CT with a single X-ray detector-row, MDCT scanners can acquire volumetric data for higher resolution

images over wider volume coverage during shorter scan times.³⁻⁵ Moreover, 8- and 16-ch MDCT scanners have been developed within the 5 years of the introduction of a 4-ch scanner. As a result of such progress in MDCT scanners, the

16-ch scanners can obtain submillimeter thickness images in the Z-direction with wider X-ray beam width. While excellent spatial resolution can be achieved in a shorter scan time with 16-ch scanners, advances in diagnostic imaging of vascular disease have not been clarified in relation to the progress in MDCT scanner development.

We compared a 16-ch MDCT scanner with 4- or 8-ch MDCT scanners with respect to the quality of CTA images reconstructed by the VR and MIP methods for visualization of TAA, AAA, and AD. A five-grade scale was used for comparison of CTAs obtained with 16-ch MDCT and those obtained with 4- or 8-ch MDCT. Mean scores were below 1 point such as 0.34, 0.43, and 0.43 for visualization of TAA, AAA, and AD respectively. These results suggest that 4- or 8-ch MDCT could provide equal diagnostic information to 16-ch MDCT on main vascular lesions. The reason for the small differences between 16-ch MDCT and 4- or 8-ch MDCT scanners may be that the width and length of the aortic lesion were sufficiently large for effective slice thickness of fewer-ch MDCT scanners,¹⁰ so that the CTA images obtained with fewer-ch MDCT scanners were as satisfactory as those obtained with 16-ch scanners. With respect to visualization of major branches, on the other hand, mean scores were 1.34 for TAA, 1.43 for AAA, and 1.29 for AD respectively. Thus, mean scores were rated above 1 point overall and these results suggested that CTA obtained with 16-ch MDCT were superior to those obtained with 4- or 8-ch MDCT scanners, while the differences between the scores of main vascular lesions and those of major branches were not significant. Since the target arteries such as branch vessels are small, 3-dimensional visualization of these arteries was directly influenced by the effective slice thickness (4-ch MDCT: 3.2 mm, 16-ch MDCT: 1.69 mm: unpublished data from GE), so that small arteries were more clearly visualized by 16-ch MDCT scanners.¹¹ This trend was more evident in CTA of pelvic/lower extremity arteries. Mean scores were 0.94 for main vascular lesion and 1.40 for branch and collateral vessels in patients with PAD, while the differences were not significant.

Concerning the delineation of major vascular lesions on coronal MPR images, mean scores were above 1 point such as 1.17 for TAA, 1.00 for AAA, and 1.00 for AD, and these

mean scores were higher than those in the assessment of CTA with VR and MIP methods. Vascular lesions are directly displayed on MPR images, so image distortion along the Z-axis is conspicuous on MPR images due to thicker effective slice thickness of a 4-ch MDCT scanner.¹² As for the delineation of major branches of the aorta on MPR images, mean scores were 1.50 for TAA, 1.43 for AAA, and 1.43 for AD. Mean scores were 1.27 and 1.40 for the delineation of main vascular lesions and branch and collateral vessels respectively, in patients with PAD on MPR images. These results were higher than in the assessment of CTAs with VR and MIP methods, and were also thought to be attributable to the thinner effective slice thickness of 16-ch MDCT scanner, while the differences were not statistically significant.

With respect to the periodic artifact at muscles and soft tissues on the CTA images reconstructed by the MIP method, the artifacts were not obvious on CTA with 16-ch MDCT. These artifacts are known as zebra artifacts and are caused by increase of noise along the Z-axis during the process of image interpolation. These artifacts tend to be especially severe off-center in the axial plane.¹³ With 16-ch MDCT, such artifacts are thought to be suppressed because axial CT images are reconstructed with consideration of the cone angle of the X-ray during image interpolation process.¹⁴ Since CT attenuation numbers are influenced by the appearance of these artifacts, it is necessary to take care when diagnosis of lesion characteristics is performed on the basis of CT attenuation numbers.

The dose of contrast medium required for 8- and 16-ch MDCT scanners for imaging the aorta was smaller than that for 4-ch MDCT scanner. Since the duration of contrast medium injection should equal the scanning time when performing CTA,¹⁵ the amount of contrast medium was smaller with 8- and 16-ch MDCT scanners because the scanning time is shorter. For CTA of pelvic/lower extremity arteries, the differences between 16- or 8-ch MDCT and 4-ch MDCT was smaller, since the scanning time from the distal abdominal aorta to the ankle is longer compared with that for the aorta. It has also been reported that the injection rate of contrast medium should be increased when scanning time is shorter.¹⁵ In the present study, however, we administered the contrast medium at a constant flow rate of 3 mL/s. This was to

minimize the effect of intravenous contrast bolus on the patient's hemodynamics and to reduce the risk of extravasation. Neither obvious hemodynamic change during injection of contrast medium nor extravasation occurred in the present series, so we could perform CTA both safely and adequately.

There are several limitations in the present study: The interval between CTAs, which was conducted multiple times in the same patient using different MDCT scanners, ranged from 1 month to 3.5 years (median: 1 year and 7 months). Therefore, the target vessels were not always in the same condition due to progression of lesions and surgical or intravascular intervention during the intervals between CTA examinations. In addition, physiological changes, such as cardiac output associated with aging, may have influenced the CTAs. In order to minimize such differences, it would be necessary to conduct CTA examinations within a short period using different models of MDCT scanners. The diagnostic capability of MDCT was not quantitatively evaluated by comparison with conventional intraarterial digital subtraction angiography, which is thought to be the gold standard for vascular imaging.

In conclusion, this study showed that MDCT is capable of acquiring volume data sets that provide excellent longitudinal spatial resolution in a shorter scan time due to the increase in X-ray detector-rows. As a result, 16-ch MDCT provides clear and artifact-free CTA images of major vascular lesions as well as PAD. Sixteen-channel MDCT was particularly superior to 4-ch MDCT with respect to the visualization of small arteries. In addition, not only the amount of contrast medium but also calculated CTDI_{vol} of the same examination distance tended to decrease as scanning time shortened, suggesting that an advanced MDCT scanner could promote further reduction in invasiveness of CT examination.

References

- 1) Hu H, He HD, Foley WD et al: Four multidetector-row helical CT: image quality and volume coverage speed. *Radiology*, 2000, **215**: 55–62.
- 2) Hayashi H, Takagi R, Ichikawa T et al: A new technology

- in spiral volumetric CT: for understanding multidetector-row CT scanner. *Japanese-Deutsche Medizinische Berichte*, 1999, **44**: 330–341.
- 3) Yamashita Y: Multidetector-row helical CT. Yamashita Y, ed. *Chu-o-Igaku-sha*, 2001.
- 4) Rubin GD, Shiau MC, Leung AN et al: Aorta and iliac arteries: single versus multiple detector-row helical CT angiography. *Radiology*, 2000, **215**: 670–676.
- 5) Hayashi H, Takagi R, Uchiyama N et al: Three-dimensional CT angiographic assessment of pelvic and lower-extremity occlusive disease using single detector-row and multidetector-row CT scanners. *J Jpn Coll Angiol*, 2001, **41**: 785–790.
- 6) Kalender WA, Seissler W, Klotz E et al: Spiral volumetric CT with single-breath-hold technique, continuous transport, and continuous scanner rotation. *Radiology*, 1990, **176**: 181–183.
- 7) Hayashi H, Kobayashi H, Takagi R et al: Spiral CT. *Clinical Imagiology*, 1996, **12**: 181–193.
- 8) Rubin GD, Dake MD, Napel SA et al: Three-dimensional spiral CT angiography of the abdomen: initial clinical experience. *Radiology*, 1993, **186**: 147–152.
- 9) Hayashi H, Kobayashi H, Takagi R et al: Three-dimensional CT angiographic assessment of vascular diseases using various postprocessing techniques: the voxel transmission and cruising eye view methods and their respective merits. *Int Angiol*, 1999, **18**: 113–121.
- 10) Yamamoto S: Image evaluation and analysis in multislice CT. In: Yamashita Y, ed. *Multidetector-row helical CT*. *Chu-o-Igaku-sha*, 2001, 26–39.
- 11) Nakayama Y, Yamashita Y: Reconstruction parameters in MPR image and three-dimensional Images. In: Yamashita Y, ed. *Multidetector-row helical CT*. *Chu-o-Igaku-sha*, 2001, 49–55.
- 12) Sato N: Artifacts. In: Yamashita Y, ed. *Multidetector-row helical CT*. *Chu-o-Igaku-sha*, 2001, 40–43.
- 13) Barrett JF, Keat N: Artifacts in CT: recognition and avoidance. *Radiographics*, 2004, **24**: 1679–1691.
- 14) Hsieh J: 10.3.2 Selection of region-of-reconstruction. In: Hsieh J, ed. *Computed tomography: principles, design, artifacts, and recent advances*. *SPIE PRESS*, 2003, 322–324.
- 15) Napoli A, Fleischmann D, Chan FP et al: Computed tomography angiography: state-of-the-art imaging using multidetector-row technology. *J Comput Assist Tomogr*, 2004, **28** (Suppl 1): S32–S45.